Chemistry–A European Journal
Research Article
doi.org/10.1002/chem.202302113
Chemistry Europe
European Chemical Societies Publishing
www.chemeurj.org

Alternating Stereospecificity upon Central-Atom Change: Dynamics of the $F^- + PH_2Cl$ S_N2 Reaction Compared to its C- and N-Centered Analogues

Anett Giricz,[a] Gábor Czakó,*[a] and Dóra Papp*[a]

Central-atom effects on bimolecular nucleophilic substitution (S_N2) reactions are well-known in chemistry, however, the atomic-level S_N2 dynamics at phosphorous (P) centers has never been studied. We investigate the dynamics of the $F^- + PH_2Cl$ reaction with the quasi-classical trajectory method on a novel full-dimensional analytical potential energy surface fitted on high-level ab initio data. Our computations reveal intermediate dynamics compared to the $F^- + CH_3Cl$ and the $F^- + NH_2Cl$ S_N2 reactions: phosphorus as central atom leads to a more indirect S_N2 reaction with extensive complex-formation with respect to the carbon-centered one, however, the title reaction is more direct than its N-centered pair. Stereospecificity, characteristic at C-center, does not appear here either, due to the submerged front-side-attack retention path and the repeated entrance-channel inversional motion, whereas the multi-inversion mechanism discovered at nitrogen center is also undermined by the deep Walden-well. At low collision energies, 6% of the PH_2F products form with retained configuration, mostly through complex-mediated mechanisms, while this ratio reaches 24% at the highest energy due to the increasing dominance of the direct front-side mechanism and the smaller chance for hitting the deep Walden-inversion minimum. Our results suggest pronounced central-atom effects in S_N2 reactions, which can fundamentally change their (stereo)dynamics.

Introduction

Bimolecular nucleophilic substitution (S_N2) is one of the most essential reaction families in organic and biochemistry. Carbon-centered S_N2 (S_N2@C) processes have been the most widely studied in the reaction family,[1–31] however, nitrogen, silicon, and phosphorus-centered S_N2 reactions have also been subject of several investigations due to their chemical and biological relevance.[32–49] S_N2 reactions in the gas phase, as many other chemical reactions, were first studied by kinetic measurements and models, revealing for example their bimolecular nature.[3–5,7,8,10] While these kinds of reactions were extensively applied in synthetic chemistry, with the quantum chemical breakthrough in the 1970s, more and more theoretical tools became available to study the physical origin behind S_N2 processes. Detailed theoretical investigations of several representative S_N2 reactions at various central atoms were performed by Bickelhaupt and coworkers by examining the energies and geometries of many transition states (TSs) and stable minima utilizing density functional theory (DFT) methods and their Activation Strain Analysis.[32,33,36,44,47,48] They revealed that C-centered S_N2 reactions feature a double-well minimum potential energy curve with a Walden-inversion TS along the reaction coordinate, however, if we switch to 3rd-row elements as central atoms, the minimum energy path will only involve a stable transition complex, turning this way into a single-well pathway.[32,33,36,44,47,48]

Nevertheless, for a deeper understanding of the complex physics and chemistry behind these reactions, a dynamical approach is crucial, since they do not necessarily follow the minimum energy path, as it was demonstrated by Hase and coworkers in the case of the $OH^- + CH_3F$ reaction.[12] Using their direct dynamics technique, which means that the forces that govern the classical motion of the nuclei are computed on-the-fly by using a quantum electronic structure program, they extensively studied C-centered S_N2 reaction dynamics, and discovered various alternative reaction mechanisms, such as stripping, rebound, hydrogen-bonded complex formation, and roundabout.[14,15,18,21] In parallel, crossed molecular beam experiments advanced by the pioneer developments of Wester and coworkers made possible for the first time to probe single collision events in S_N2 reactions,[14] leading to a fruitful cooperation between theory and experiment. However, two hindering factors prevented direct dynamics calculations from achieving quantitative agreement with experiments: (a) the high computational demand of gradient calculations allows only for using lower levels of theory (DFT or second-order

[a] A. Giricz, Prof. Dr. G. Czakó, Dr. D. Papp
MTA-SZTE Lendület Computational Reaction Dynamics Research Group
Interdisciplinary Excellence Centre and
Department of Physical Chemistry and Materials Science
Institute of Chemistry, University of Szeged
Rerrich Béla tér 1, Szeged H-6720 (Hungary)
E-mail: gczako@chem.u-szeged.hu
dorapapp@chem.u-szeged.hu
Homepage: http://www2.sci.u-szeged.hu/czako
http://www.staff.u-szeged.hu/~pappdo

Supporting information for this article is available on the WWW under https://doi.org/10.1002/chem.202302113

Møller-Plesset perturbation theory (MP2)), and (b) even then, only a few hundred trajectories can be computed.

In the early 2010s our group introduced a different approach to model the dynamics of S_N2 reactions: we develop full-dimensional analytical potential energy surfaces (PESs)[17,19,24] by fitting a permutationally invariant polynomial function[50] on a few tens of thousands of high-level (usually coupled-cluster/triple-zeta-quality)[51,52] ab initio energy points. Such a PES then allows for computing millions of quasi-classical trajectories (QCT), thereby massively reducing statistical error. While the electrons are treated with state-of-the-art quantum-mechanical electronic structure methods when constructing the PES, in QCT we treat the much heavier nuclei with Newtonian mechanics, which provides good description of their motion during a chemical reaction, most often in excellent agreement with experiments.[20,24,27] Quantum dynamics simulations, especially in full dimensions, are still limited to only few-atomic systems.[16,22,23,53] The prefix "quasi", however, refers to some quantum spirit encompassed in QCT: our classical trajectories always start from a well-defined rovibrational quantum state of the reactants. Quite recently, the development of the above-mentioned analytical PESs has been automatized in our group with the ROBOSURFER program package.[54] This way, we have been able to successfully study the dynamics of 5–10 atomic systems, even on highly-structured global reactive PESs,[27,39,46,55] and reveal novel, sometimes low-probability reaction routes. Such an approach made possible to uncover new mechanisms, for example, double inversion[19] and oxide-ion substitution[28] in C-centered, and a multi-inversion pathway[46] in N-centered S_N2 reactions, as well as an unexpected leaving-group effect[20] and to successfully identify a bimolecular elimination (E2) channel[27] in joint experimental and theoretical studies.

As outlined above, S_N2@C, serving as a prototype of polyatomic ion-molecule reactions, has been widely investigated in the past decades, both by experimental and theoretical means, resulting in the extension of our fundamental text-book knowledge of the Walden-inversion[1,2] and front-side-attack[2] reaction routes. Much less, but literature is still available on S_N2 reactions occurring at the valence-isoelectronic Si-center, revealing important deviations from C-center: the nuclear arrangement, where Walden inversion takes place does not correspond to a transition state, but to a minimum on the PES, caused by stronger ligand-central atom bonds and smaller steric congestion effects.[32–39,47] Furthermore, the barrier to front-side attack, resulting in products with retained configuration, has been found to be submerged below the energy of the reactants, which can compromise the stereoselectivity of S_N2@Si. In addition, partly due to the weaker Si–H bond, various alternative product channels can emerge in S_N2@Si.[38,39]

An interesting question arises when comparing C- and N-centered members of the S_N2 family: how does the possibility of inversion around the central atom affect the dynamics, especially the stereodynamics of the N-centered S_N2 reaction? Recently, we have answered this question based on a detailed QCT study performed on a high-quality PES: a novel reaction mechanism, called *multi-inversion*, has been unveiled, which is prevalent at lower collision energies and fully undermines the stereoselectivity of the $F^- + NH_2Cl$ reaction.[46] This pathway involves a recurring inversional motion through a low-energy submerged $[FH\cdots NHCl]^-$ TS in the entrance channel, while the effect of self-inversion of the reactant, despite having a low energy barrier, has turned out to be less significant.

Following this train of thought, we arrive at the next intriguing question: how will the stereodynamics unfold in the case of a phosphorus-centered S_N2 reaction, where a similar qualitative potential energy profile was revealed as for S_N2@Si (Walden minimum and submerged front-side TS),[36,47–49] but configuration inversion of the reactants and products (although trough a higher barrier,[56] than at N-center) is also possible? Taking a big step from previous stationary-point studies on S_N2 central-atom effects,[33,36,38,40,44,45,47–49] in the present article, for the first time, we shed light on the in-depth dynamics of the $F^- + PH_2Cl$ reaction on a newly-developed high-level ab initio full-dimensional analytical PES, with a special emphasis on stereodynamics. Besides the fact that P-centered S_N2 reactions are found to play an essential role in biochemical processes,[57–59] the title reaction is also expected to be an ideal prototype to address the above central-atom question at the deepest, atomic level. We present a thorough comparison with the dynamics of the N- and C-centered analogous reactions, previously investigated in detail in our group,[17,19,20,24,45,46] where qualitative differences and their background are targeted.

Results and Discussion

Energetics

As an initial step of our investigation, we map the PES of the $F^- + PH_2Cl$ reaction using the best available ab initio electronic structure methods (see Computational details) completing this way the first detailed accurate analysis of the energetics of the title reaction. We identify product channels of a wide energy range and numerous stationary points characteristic of various reaction mechanisms. The two most important reaction channels of this (and many other) ion-molecule reactions, S_N2 and proton-transfer, and the corresponding minimum and transition-state geometries, determined at the CCSD(T)-F12b/aug-cc-pVTZ level of theory, and benchmark energies, including basis-set convergence-, core-correlation- and zero-point vibrational energy (ZPVE) corrections, are shown in Figure 1. Relative energies for all geometries including the higher-energy products, computed at various levels of theory along with the auxiliary energy correction values are presented in Table S1 of the Supporting Information (SI).

Taking a look at Figure 1, the first thing we might notice is the extremely deep Walden-minimum at −58.3 kcal/mol relative energy with respect to the reactants, which connects directly the reactants with the products leaving the back-side-attack pathway without pre- and post-reaction complexes or TSs. It is also important to highlight that the geometry corresponding to the Walden-complex is markedly product-like. The next interesting features of the schematic PES of Figure 1, referring to stereochemistry, are the self-inversion barriers: 43.8 and

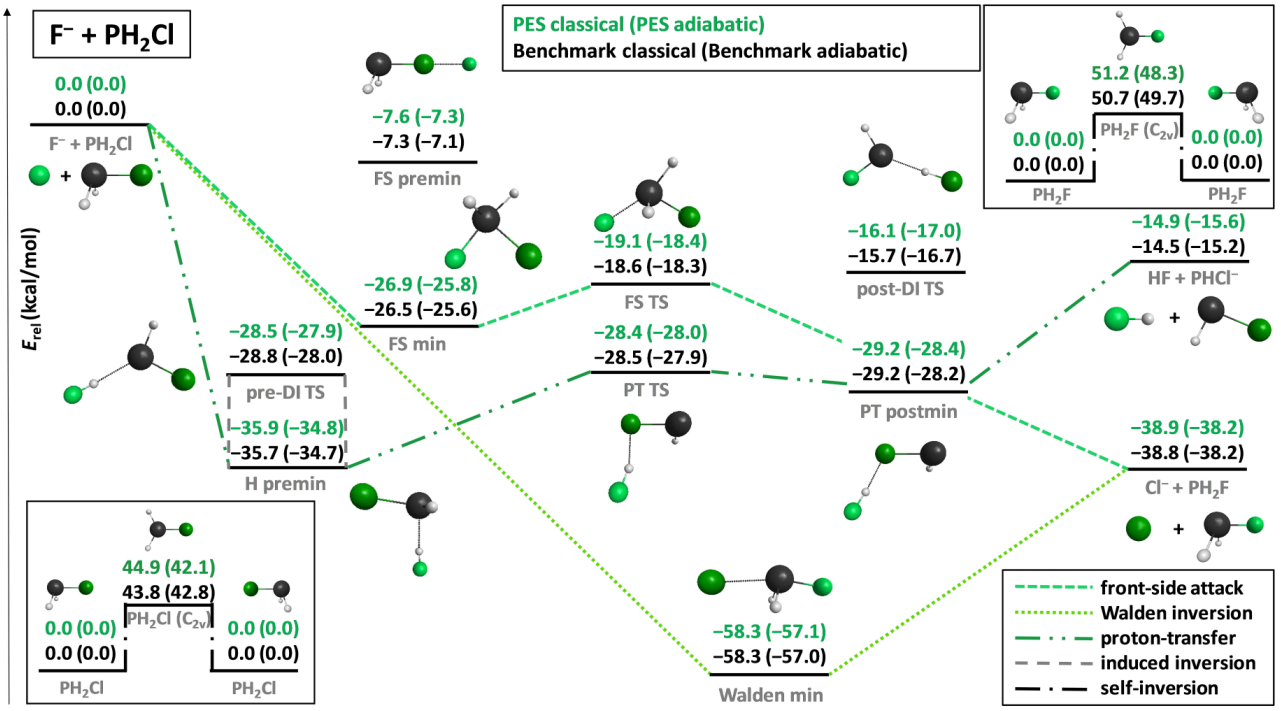

Figure 1. Schematic potential energy diagram of the $F^- + PH_2Cl$ reaction, comparing classical and adiabatic relative energies (given in kcal/mol) of the stationary points obtained with high-level ab initio methods (benchmark) with those determined on the PES, as well as showing various possible reaction mechanisms.

50.7 kcal/mol for the reactant (PH_2Cl) and the product (PH_2F) molecules, respectively. These values are much higher than the corresponding ZPVEs (11.7 and 12.4 kcal/mol, respectively), therefore, even despite the presence of potentially highly-excited products due to the substantial S_N2 reaction energy (−38.8 kcal/mol), we cannot expect self-inversion to occur, because it is only moderately relevant even in the case of the analogous N-centered reaction,[46] which had 8.8 and 15.3 kcal/mol high barriers for the self-inversion process of the reactant and the product, respectively. Additionally, even at higher collision energies the excess translational energy is not likely to be transferred into the inversional vibrational degree of freedom (umbrella motion) of the reactant or the product with the required efficiency.

As can be seen in Figure 2, in the case of the $F^- + CH_3Cl$ reaction, stereospecificity is not affected significantly, because the lowest-energy Walden-inversion pathway does not really interfere with the high-lying retention pathways, front-side attack and double-inversion.[19] By contrast, there are several reasons for the $F^- + NH_2Cl$ reaction not be stereo-selective, based purely on its energetics, as also outlined in Figure 2: the deep H-bonded minimum, the only one in the entrance channel, and the corresponding low-lying inversional TS with a $[FH\cdots NHCl]^-$-like structure induce a recurring change in the reactant configuration.[46] This, supplemented with the occasional (self- or induced) inversion of the highly-excited product molecules culminates in a new reaction mechanism, discovered in our group and called *multi-inversion*, which dominates this S_N2@N reaction at low collision energies thereby undermining its stereospecificity.[46]

In the case of the $F^- + PH_2Cl$ reaction the deep Walden-inversion minimum is expected to have a major effect on the dynamics, and, obviously, on stereo-selectivity as well. Here we have a H-bonded pre-reaction minimum 36 kcal/mol below the reactants, with a corresponding 7 kcal/mol-high 'pre-double-inversion' pre-DI TS (DI is rather a traditional name)[19] which is challenged to be able to compete with the attractive force of the global Walden-inversion minimum. Another important feature of the Walden-minimum is that it is asymmetric, that is, −58 kcal/mol deep relative to the energy of the reactants, but it is much closer in energy to the products with only a 19.5 kcal/mol difference. Along with its product-like geometry, it is expected that it will readily channel the reactants into products, like a slipway. Based on the stationary-point energies, since we have not found the H-bonded minimum in the exit channel (our attempts always converged to the Walden-minimum structure), and the post-DI TS also lies quite high in energy, stereodynamics is not foreseen to be strongly affected once the substitution took place. Interestingly, the PES of the title reaction, similarly to its N-centered analogue, lacks both the pre- and post-reaction ion-dipole minimum, which are essential in governing the S_N2 pathway at C-center.[17,19] Another possible way for the PH_2F product to form in retained configuration may be the front-side-attack route, along which the stationary points are also located well below the reactants, which is a striking contrast to the N- and C-centered analogous reactions, where the front-side barriers were found above 30 kcal/mol relative

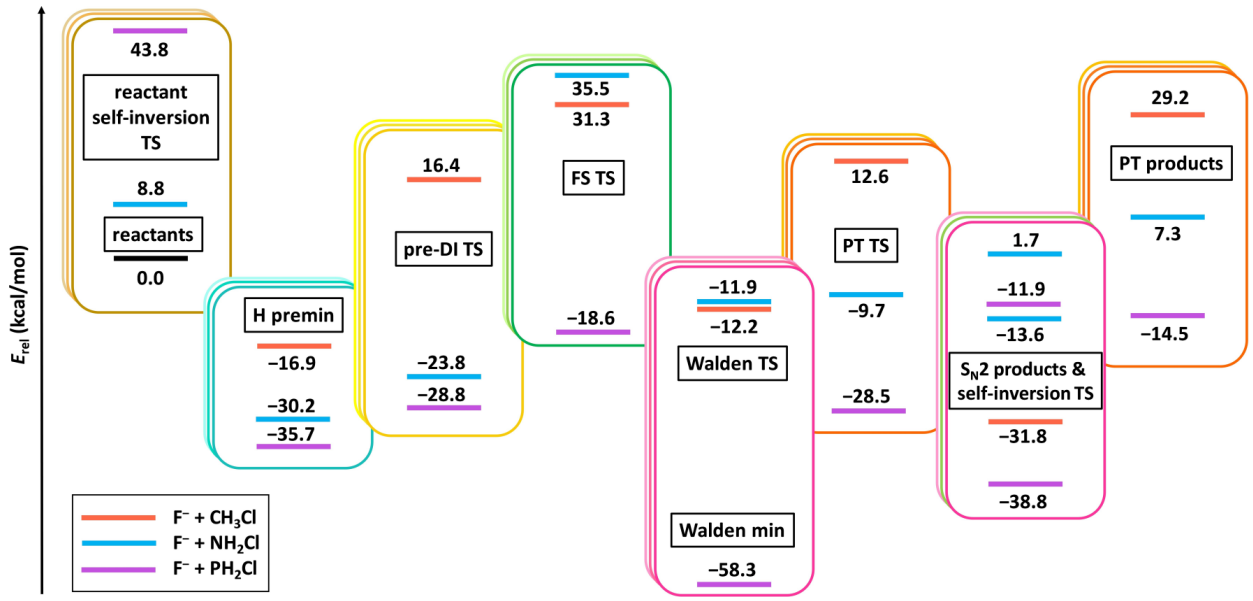

Figure 2. Benchmark classical relative energies of some representative stationary points of the $F^- + CH_3Cl$ (orange lines),[19] the $F^- + NH_2Cl$ (blue lines),[45,46] and the $F^- + PH_2Cl$ (purple lines) reactions.

energy (Figure 2).[19,45,46] Moreover, at P-center we also find a new front-side minimum at −26.5 kcal/mol. Here, the existence of a multi-inversion mechanism is also in question, because from H premin proton-transfer (with a −28.5 kcal/mol TS) is energetically equally favorable as the induced inversion through pre-DI TS (−28.8 kcal/mol), in contrast to the observations for the N-centered reaction, where induced inversion is more likely to occur than PT after the system hitting the global H-bonded minimum (see Figure 2).[46] Nevertheless, the possibilities of both the repeated inversion of PH_2Cl and the barrierless front-side-attack pathway could compromise the stereospecificity of the title reaction.

In the C-centered analogous reaction, the relatively shallow minima and low TSs along the only barrierless Walden-inversion route guide the reactants all the way to the products, while both the retention and the (highly endothermic) proton-transfer reaction paths are located quite far in energy, which results in fast-proceeding dynamics of that S_N2@C reaction.[20] In stark contrast to this, in the N-centered reaction the deep minima and TSs, as well as the more competitive proton-transfer pathway lead to very indirect dynamics.[46] From Figure 1 it is clear that all the $F^- + PH_2Cl$ reaction routes lack both kinetic and thermodynamic barriers, and here the FS premin structure with its non-reactive orientation is the highest-lying stationary-point along the reaction coordinate, this way it may hinder the reaction less, than at N-center, where it has similar relative energy as the PT and Walden TSs.[46] Although the exothermicity of the PT channel at P-center could make it somewhat more competitive with S_N2, it is most likely to impede the front-side pathway, since the PT TS and postmin lie much higher in energy with respect to the Walden-inversion path than at N-center, and thus much closer to the FS pathway (at C-center PT is endothermic, and also has a positive barrier).

Based on the above assumptions, which were derived merely from the energetics of the title reaction, one might wonder how it will actually proceed in the presence of an almost 60 kcal/mol deep Walden-inversion minimum with competing proton-transfer and S_N2 retention routes. To both the stereo-selectivity- and mechanism-related questions only an accurate and detailed dynamical investigation can give answers.

PES and dynamics

To be able to study the dynamics of the title reaction, we have developed a full-dimensional global analytical PES fitted on 21 212 geometries and the corresponding ab initio energies, determined at the highest available level of theory, eliminating also the occasional breakdown of the gold-standard CCSD(T) method,[60] using a permutationally invariant polynomial technique.[50] The excellent accuracy of the fitting can be seen from the values of Figure 1: the stationary-point energies, both classical and adiabatic, obtained on the PES differ only by a few 0.1 kcal/mol from the benchmark values, except for the high-energy self-inversion barriers, where the deviation is about 1 kcal/mol. The overall root-mean-square error of the final fit is 1,07 kcal/mol in the 0–63 kcal/mol (0–0.1 hartree) energy interval relative to the global minimum (Walden min) of the fitting set, which provides chemical accuracy for the dynamical investigation.

The reactivities of the S_N2 and PT channels of the $F^- + PH_2Cl$ reaction compared to those of the C- and N-centered analogous processes are shown in Figure 3. A *hard* ZPVE-constraint is applied in case of the PT reaction at N- and P-center (at C-center it has negligible reactivity with respect to the other two PT channels), which is a usual tool to get more realistic results by discarding those trajectories that give one (or both) of the

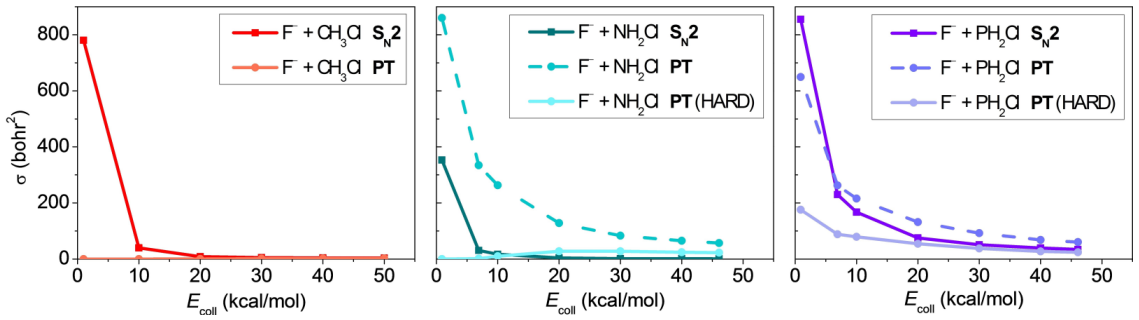

Figure 3. Integral cross sections as a function of collision energy for the S_N2 and proton-transfer (PT) channels of the $F^- + CH_3Cl$,[19,22] the $F^- + NH_2Cl$,[46] and the $F^- + PH_2Cl$ reactions. The PT curves obtained with *hard* ZPVE-constraint (the classical vibrational energy of each product must be larger than its own ZPVE) are also shown, where relevant.

product(s) with vibrational energy lower than their ZPVE(s). This way the well-known ZPVE-leakage issue of QCT is passively treated. The excitation functions of Figure 3, that is, the integral cross sections as a function of the collision energy, feature a monotonically decaying shape for all three S_N2 channels, as well as for some of the PT curves, however the hard-constrained $F^- + NH_2Cl \rightarrow HF + NHCl^-$ reactivity has a small maximum and a threshold due to its endothermicity. Likewise, exothermicity is the reason why the ZPVE restriction does not change the shape of the P-centered PT excitation function: $PHCl^-$ products excited by the reaction energy are less likely to violate the ZPVE-constraint. However, behind the monotonic decay is not only the exothermicity, but also the lack of barriers: decreasing collision time with increasing initial translational energy is the main hindering effect in such reactions, which prevents the interaction between the reactants to develop. The S_N2 reactivity is generally very high for all three reactions, with the smallest values for $F^- + NH_2Cl$, where PT is the most competitive, and even outperforms S_N2 at higher energies. In the $F^- + PH_2Cl$ reaction, as expected based on the energetics, PT, despite its exothermic nature, turns out to be less competitive with S_N2 than at N-center, due to the larger gap between its energy path and that of Walden-inversion, however, it is still close to the FS route in energy. Excitation functions of lower-reactivity product channels along with more ZPVE-restricted PT results are shown in Figures S1 and S2 of the Supporting Information.

In Figure 4 the results of the detailed dynamical analysis of the $F^- + PH_2Cl \rightarrow Cl^- + PH_2F$ reaction are shown. We can notice that the lowest-energy opacity function has a markedly different shape with a maximum at larger *b* impact parameters (upper left panel). Also, the maximum value of *b*, where we observe reactivity is far the largest, 25 bohr, for the lowest collision energy, demonstrating the promoting effect of reaction time for barrierless exothermic reactions. At higher energies b_{max} is between 9–15 bohr with opacity functions of decaying shapes featuring shoulders and local maxima, which, together with the scattering angle distributions of the products (upper right panel), showing an increasing forward-scattering preference with increasing collision energy, refer to a slightly more dominant stripping mechanism preferred at large impact parameters, where the incident F^- ion strips away the PH_2 part of the reactant molecule and leaves keeping its initial direction. The high probabilities at smaller *b* values at low collision energies, however, favor a backward-scattering direct rebound mechanism, also reflected in the scattering angle distributions. The PH_2F internal energy distributions and relative translational energy distributions of the products are also plotted in Figure 4 (lower panels), from which information about the directness of the reaction can be deduced. At lower collision energies the internal energy curves peak near the maximum available energy (released reaction energy + reactant ZPVE + collision energy), which indicates complex-formation-mediated dynamics, where the excess energy is trapped in the internal degrees of freedom and the products separate with only minimal translational energy.

As the initial translational energy increases, it flows less into the internal degrees of freedom and more into product recoil, which is clearly manifested in the internal-energy distributions as well, which no longer peak around the maximum available energy and have more and more Gaussian-like shapes, while the translational energy curves widen and their maxima blue-shift. From this pattern, a picture of an increasingly direct reaction emerges with increasing collision energy, while more indirect dynamics proceeding through pre- and postreaction minima can be inferred at lower collision energies. From the internal energy distribution of PH_2F, it can also be seen that only a negligible amount of the S_N2 trajectories are ZPVE-violating. Similar detailed results for the PT reaction, which reveal lower probabilities and much more direct dynamics, can be found in Figure S3 in Supporting Information.

In Figure 5 the S_N2 integral cross sections are divided into inversion and retention curves, and the retention/inversion ratio is also plotted in the insets. Besides the generally higher S_N2 reactivity, we find much more inverted products formed in the $F^- + PH_2Cl \rightarrow Cl^- + PH_2F$ reaction, than in the N-centered analogue. However, as collision energy increases the ratio of the products with retained configuration increases at P-center: from the lowest-energy 6% it reaches 24% at the highest energy. Note, that while in the P-centered case the S_N2 reaction has a 34.3 $bohr^2$ cross section even at the highest collision energy, the reactivity of the $F^- + NH_2Cl \rightarrow Cl^- + NH_2F$ reaction exceeds 10.0 $bohr^2$ only below 10 kcal/mol, where it features a decreasing retention ratio with increasing energy, falling in the 48–36% interval, indicating a near racemic outcome of this reaction

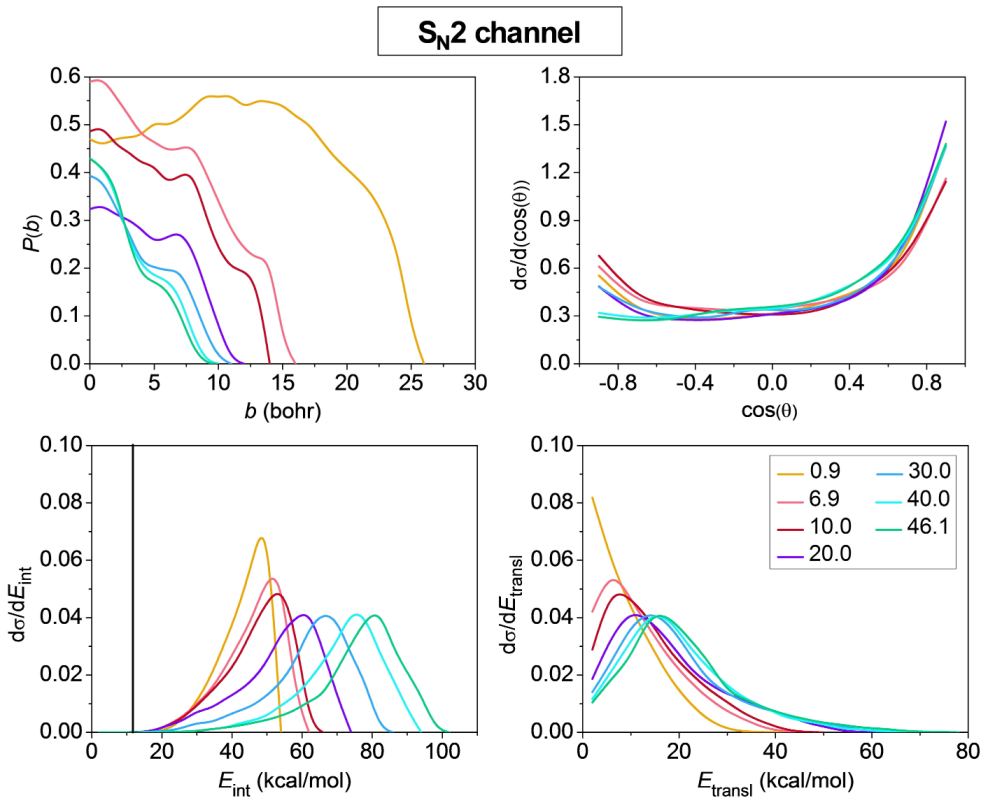

Figure 4. Opacity functions (upper left panel), product scattering angle (upper right panel), PH_2F internal energy (lower left panel) and product relative translational energy (lower right panel) distributions for the $F^- + PH_2Cl \rightarrow Cl^- + PH_2F$ S_N2 reaction obtained at different collision energies (denoted with different colors and given in kcal/mol), without ZPVE constraint. The vertical black line indicates the ZPVE of PH_2F.

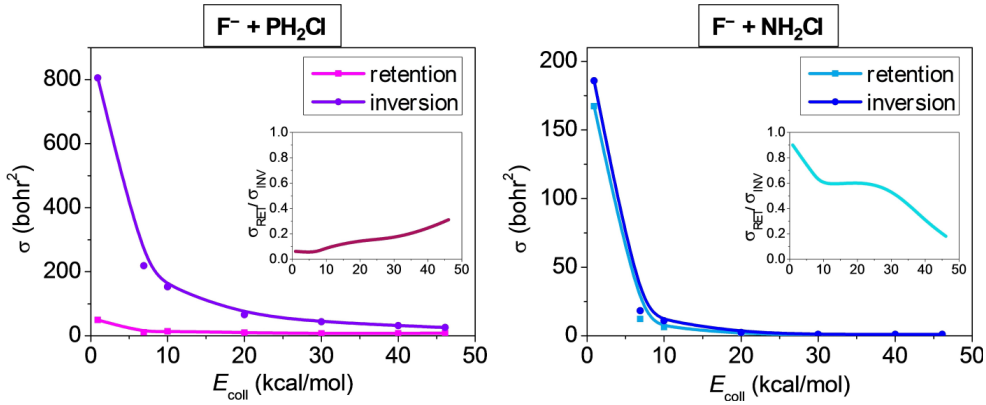

Figure 5. Retention and inversion integral cross sections for the $F^- + PH_2Cl \rightarrow Cl^- + PH_2F$ and the $F^- + NH_2Cl \rightarrow Cl^- + NH_2F$ (Ref. [46]) reactions, with their ratios shown in the insets, as a function of collision energy.

at the lowest energies, where the reactivity is the highest, attributed to the *multi-inversion* mechanism guided by the H-bonded entrance-channel complex and inversion TS.[46] On the contrary, the S_N2 reaction at P-center is almost stereospecific at the lowest energies, but an increasing ratio of PH_2F products with retained configuration is observed as collision energy increases. Here, we also check non-reactive trajectories, and find the ratio of inverted reactants absolutely negligible at all energies, also in contrast to the N-centered reaction, where collision-induced inversion is of major significance.[46] Since the stereochemical behavior of the N- and P-centered reactions turns out to be quite opposite, we are curious about what circumstances shape the course of the P-centered S_N2 reactions, with particular regard to the retention trajectories.

Reaction mechanisms and stereochemistry

We visualize a few hundred quasi-classical trajectories to be able to follow the title reaction step by step from reactants to

the products, just as a molecular movie. A few selected trajectories can be viewed in the Supporting Information. First, we inspect S_N2 trajectories that result in PH_2F with the same configuration as the PH_2Cl reactant. At lower collision energies we can distinguish between three different mechanisms for these retention trajectories: (1) *direct front-side*: the substitution takes place through FS TS without significant complex formation, (2) *complex-forming multi-inversion*: the F^- ion abstracts a proton multiple times, and HF is roaming around the $PHCl^-$ unit, while the system might even hit the PT postmin structure, then, after the proton is put back, the substitution proceeds through either FS TS or the Walden-minimum, sometimes being stuck in the latter arrangement, (3) *post-Walden double-inversion*: the substitution occurs in the Walden-minimum, but the Cl^- ion does not drift away, and while it is roaming around the PH_2F unit it abstracts a proton, and then puts it back on. (This post-reaction proton abstraction can, of course, happen multiple times, resulting occasionally in inversion of the original configuration). This latter mechanism is not expected based on the stationary-point energies, since it does not happen through the post-DI TS, but by Cl^- abstracting a proton. We can see that complex-formation is highly involved in the low-energy retention trajectories, and it is also significant in the collisions that end up with inverted S_N2 products: the abstraction of a proton from PH_2Cl or PH_2F is quite frequent, which can be explained by the weaker P–H bonds with respect to bonds between second-row central atoms and hydrogen. In contrast to the extensive complex-formation experienced for S_N2 trajectories, proton transfer is found to be proceeding more directly, in accordance with the more direct dynamics indicated in Figure S3 in Supporting Information.

Regarding a random bunch of trajectories visualized, what is seen at low collision energies is that the first step of several collisions seems to be the immediate 'falling into' the Walden-minimum, followed by a quick rebound of the F^- ion due to the large energy gained in the almost 60 kcal/mol deep Walden-well. It is also quite usual that the rebounded F^- ion drifts 6–8 Å away from the PH_2Cl unit, and approaches it from there again. After that, both a proton transfer and a substitution can occur, in the latter case most of the reaction time being spent near the Walden minimum, whereas several roaming events of HF can also be observed. The forming of a hydrogen-bond or proton transfer can also often be the initial step of the trajectories, followed by various possible events.

As we increase collision energy, only one amongst the above three retention S_N2 mechanisms survives: the direct front-side substitution. The front-side pathway ensures a more direct course of the reaction as it is the highest-energy reaction route with the smallest chance for the system to stick in deep minima. At the same time, with increasing collision energy the system tends to avoid the deep Walden-minimum more and more, as the decreasing collision time no longer supports complex formation. These shifts in the S_N2 mechanisms result in the reduced ratio of the inversion events at higher energies in accordance with the excitation functions of Figure 5. Another interesting observation at the highest energies is that, as the shallowest minimum, the non-reactively oriented FS premin also plays a significant role: it causes repulsion between the reactants, diverting them from each other, this way contributing to decreasing reactivity (Figure 3).

As seen from the scattering-angle distributions of Figure 4 higher energies clearly favor forward-scattering, whereas at lower energies backward scattering also turns out to be significant. As is well known, the pre- and post-reaction-complex-mediated mechanisms observed at the lower collision energies lead to random-direction scattering, because the reacting partners loose information about their initial direction during complex-formation. Thus, the specific mechanisms of the direct reaction pathways will determine the scattering preference. Typically, both Walden-inversion and front-side attack can proceed through either direct-rebound or stripping mechanisms, and Walden-inversion can lead to either backward- or forward-scattered products, for example, at large impact parameters and high collision energies, when the PH_2Cl molecule turns towards the fast incident F^- ion before the reaction and lets it keep its initial direction. In fact, for both the inversion and the front-side pathways, the stripping mechanism will be favored at higher collision energies, where the centrifugal barrier caused by large impact parameters, preferring direct stripping, can be overcome. Nevertheless, a front-side substitution is very unlikely to result in a backward-scattered product, because even upon a direct rebound process, the front-side TS will favor sideways scattering owing to its characteristic geometry. Thus, since in the case of the title reaction the preference for large-*b* reactivity is not pronounced at higher collision energies (as seen in the opacity functions of Figure 4), the shift from backward to forward scattering with increasing collision energy can be attributed to the increasing ratio of direct front-side S_N2 reactions along with the decreasing contribution of indirect complex-forming dynamics.

Overall, regarding both the stereospecificity and the directness of the dynamics, the title S_N2 reaction shows an intermediate behavior compared to its C- and N-centered analogues: it does not show the stereospecific behavior, which is characteristic at C-center, but it is also very far from producing a racemic mixture of products, as seen at N-center, stemming from the *multi-inversion* mechanism. An alternating stereospecificity is revealed when moving from the usual C-centered S_N2 reaction to N-center, and then to phosphorus as central atom. The deep Walden-minimum, being asymmetric both along the energy and the reaction coordinate axes, primarily affects the dynamics of the $F^- + PH_2Cl \rightarrow Cl^- + PH_2F$ reaction, as do the submerged front-side barrier and the exothermic PT channel. However, due to the rather high-lying PT stationary points relative to the Walden-inversion complex and the barrierless nature of the energetically closer front-side reaction, proton-transfer is found to be not as competitive with the S_N2 path here as in the N-centered reaction. These above observations, and the lower chance for complex-formation and for recurring inversion in the entrance-channel near the H-bonded premin and TS geometries, make the P-centered S_N2 reaction more direct, especially at higher collision energies, than the one with N as central atom. On the contrary, $S_N2@P$ is found to be less direct compared to $S_N2@C$, where proton-

transfer is highly endothermic and the entrance channel features a less deep H-premin with a 33 kcal/mol high double-inversion TS. Taken together, very rich dynamics is found for the $F^- + PH_2Cl \rightarrow Cl^- + PH_2F$ reaction with strong collision-energy dependence and various mechanisms, leading to somewhat restored stereospecificity at low energies with respect to S_N2@N, which, however, is undermined at higher collision energies.

Conclusions

Quasi-classical trajectory studies on analytical potential energy surfaces of prototypic ion-molecule reactions, such as the title reaction, are the best available theoretical methods to uncover their atomic-level mechanisms and investigate the stereodynamics of their S_N2 routes. In this work we aim to unveil the effect of the change of central atom in such ion-molecule reactions by comparing the dynamics of the $F^- + PH_2Cl$ reaction with its carbon- and nitrogen-centered analogues, taking a big step forward from previous stationary-point studies. After mapping the complex potential energy surface of the $F^- + PH_2Cl$ system using high-level ab initio methods, we develop an accurate global full-dimensional analytical PES and investigate the dynamics of the title reaction in detail. A deep Walden-inversion minimum, a relatively high-lying proton-transfer channel, a submerged front-side attack pathway, and high self-inversion barriers mediate the course of the reaction, along with the presence of a low-lying H-bonded minimum and transition state in the entrance channel, the latter being responsible for the *multi-inversion* mechanism at N-center. The P-centered S_N2 reaction turns out to be more indirect and less stereospecific, than its C-centered pair, due to the more significant contribution of proton-transfer and retention pathways in the former case. Nevertheless, the title reaction still produces a high ratio of products with inverted configuration compared to the N-centered reaction at low energies, which, however, decreases with increasing collision energy. The phosphorus central atom also makes the S_N2 reaction more direct than nitrogen, due to the extremely deep asymmetric Walden-well with a product-like minimum geometry, the less competitive proton-transfer channel, the barrierless front-side-attack path and the less deep H-bonded entrance-channel minimum and TS. At lower collision energies extensive complex-formation can be observed both for retention and inversion trajectories, with especially long time spent near the Walden-inversion minimum; whereas with increasing collision energy direct front-side attack becomes the prevalent mechanism of the increasingly present retention S_N2 route, while the system tends to avoid more and more the deep Walden-well. These findings shed light on dynamical central-atom effects in S_N2 reactions thereby extending our knowledge of this reaction family of fundamental importance, along with hopefully motivating new theoretical and experimental investigations of even more complex ion-molecule systems.

Computational details

The final geometries of the stationary points of the reactive PES of the title reaction are determined at the explicitly correlated CCSD(T)-F12b/aug-cc-pVTZ level of theory,[52,61] and further single-point computations at these geometries are carried out to provide stationary-point energies of sub-chemical (< 1 kcal/mol) accuracy: basis-set convergence error is made negligible by performing CCSD(T)-F12b/aug-cc-pV5Z computations,[52,61] and the correlation of the core (sub-valence-shell) electrons is also taken into account at the AE-CCSD(T)/aug-cc-pwCVTZ level of theory.[51,62] For the adiabatic zero-point vibrational energy (ZPVE) correction, harmonic frequencies are also determined at the CCSD(T)-F12b/aug-cc-pVTZ level of theory.[52,61] For all electronic structure computations the Molpro software package[63] is used.

As a first step of constructing the full-dimensional PES, we generate a few thousands geometries by randomly displacing the Cartesian coordinates of the CCSD(T)-F12b/aug-cc-pVTZ stationary-point structures in the 0.0–0.4 Å interval. In the case of the reactants and products we also scatter the ion or the diatomic molecule randomly around the polyatomic moiety in the 2.5–15.0 Å distance range. Then these geometries are subjected to CCSD(T)-F12b/aug-cc-pVTZ single-point energy computations, and this initial set becomes the starting database for improving the PES with the Robosurfer program package, previously developed in our group.[54] In Robosurfer the hard upper energy limit is set to 150 kcal/mol with respect to the energy of the reactants. In a 60 kcal/mol interval above the reactant asymptote we demand a 0.5 kcal/mol fitting accuracy. For fitting the ab initio energy points Robosurfer uses a permutationally-invariant polynomial function[50] of the $y_{ij} = \exp(-r_{ij}/a)$ Morse-type variables, where r_{ij} are the interatomic distances and the a parameter, which ensures the appropriate asymptotic behavior of the PES, is set to 3 bohr for such an anionic system. The sixth-order polynomial fit, requiring 4285 coefficients, is performed using a weighted least-squares procedure, where a given energy E relative to the global minimum of the fitting set has a weight of $(E_0/(E_0+E))\times(E_1/(E_1+E))$ with $E_0 = 0.1$ hartree and $E_1 = 0.5$ hartree. In order to improve the PES, Robosurfer extracts geometries of quasi-classical trajectories run using the actual surface, which are then subjected to careful similarity-checks and undergo various screening procedures[54] before they qualify worthy of electronic-structure computation, carried out automatically with Molpro,[63] and then they are added to the fitting set. This scheme is repeated until the desired accuracy of the PES is reached. At the beginning of the PES development we chose the gold-standard CCSD(T)-F12b/aug-cc-pVTZ level of theory for single-point energy computations, but after a number of Robosurfer iterations we realized that we had encountered an electronic structure problem involving the breakdown of the (T) computations, to which a solution has already been proposed in our group,[60] thus we switched to the following composite method, which replaces the problematic standard (T) part with a correction term computed using the Brueckner-type coupled-cluster method,[64] but retains the advantages of the F12 method, providing energies as:

$$E[\text{CCSD-F12b/aug-cc-pVTZ}] + (E[\text{BCCD(T)/aug-cc-pVTZ}] - E[\text{BCCD/aug-cc-pVTZ}]) \quad (1)$$

After restarting the PES development with the above composite method, we run trajectories at the following collision energies with the maximum values of the impact parameter (distance of the velocity vectors of the reactants given in bohr) shown in parentheses: 1.0 (25.0); 10.0 (10.0); 20 (6.0); 30 (6.0); 40 (6.0); 50 (6.0); 60 (6.0) and 60 (3.0) kcal/mol through 75, 7, 21, 20, 8, 61, 52

and 50 ROBOSURFER iterations, respectively. The final PES is obtained by fitting 21 212 composite ab initio data points.

To investigate the dynamics of the $F^- + PH_2Cl$ reaction we run quasi-classical trajectories at collision energies (E_{coll}) of 0.9; 6.9; 10.0; 20.0; 30.0; 40.0 and 46.1 kcal/mol, which are the same values as those applied in the case of the $F^- + NH_2Cl$ reaction.[46] The orientation of the reactants is random, and their ZPVE is set using standard normal-mode sampling[65] before initiating the trajectories. The distance of the center of masses of the reactants is $\sqrt{x^2 + b^2}$, where $x = 30.0$ bohr and the b impact parameter is varied between 0 and b_{max} (the value of b where the reaction probability vanishes) with a step size of 1.0 bohr. 5000 trajectories are run at each b-E_{coll} combination, thus we run more than half a million trajectories overall. All the trajectories are propagated with a 0.0726 fs time step until the largest interatomic distance becomes 1.0 bohr larger than the largest initial one.

Integral cross sections for each reaction channel are calculated as a b-weighted numerical integration of the $P(b)$ opacity functions (the P reaction probability as a function of b). In the case of the proton-transfer channel we applied three types of ZPVE-restriction on the products of the trajectories: (1) *soft*: the sum of the classical vibrational energy of $PHCl^-$ *and* the internal energy of HF must be larger than the sum of the harmonic ZPVE of $PHCl^-$ *and* the anharmonic ZPVE of HF corresponding to its actual rotational state. Variationally-determined rovibrational states of HF are taken from Ref. [66]. (2) *hard*: the previous conditions must be true for each product separately, (3) *PHC^--only*: the constraint is applied only for the polyatomic product. The scattering angle distributions of the products are obtained by binning the cosine of the included angle θ of the relative velocity vectors of the products and the reactants into 10 equidistant bins from -1 to 1. $\theta = 180^\circ$ corresponds to backward scattering. The configuration of the PH_2Cl molecule (which is also the product of non-reactive collisions) and the PH_2F product molecule is identified as retained (retention) if the sign of the scalar product of the normal vector of the HPH plane and the PX (X = Cl, F) vector is the same as in the initial reactant configuration, otherwise it is assigned as inverted (inversion).

Supporting Information

Details of the J_{HF} quantum number assignment, relative energies of the stationary points of the $F^- + PH_2Cl$ reaction obtained at different levels of theory, integral cross sections for the proton-transfer channel determined applying different zero-point energy constraints, integral cross sections of low-probability product channels, and detailed dynamical analyses of the proton-transfer channel (PDF) as well as stationary-point geometries and energies on the PES (TXT) and animations of representative trajectories (AVI).

Acknowledgements

This work was supported by the National Research, Development and Innovation Office–NKFIH, K-125317; project no. TKP2021-NVA-19, provided by the Ministry of Innovation and Technology of Hungary from the National Research, Development and Innovation Fund, financed under the TKP2021-NVA funding scheme; and the Momentum (Lendület) Program of the Hungarian Academy of Sciences.

Conflict of Interests

The authors declare no conflict of interest.

Data Availability Statement

The data that support the findings of this study are available from the corresponding authors upon reasonable request.

Keywords: bimolecular nucleophilic substitution · phosphorus center · potential energy surface · reaction dynamics simulations · stereochemistry

[1] P. Walden, *Ber. Dtsch. Chem. Ges.* **1896**, *29*, 133–138.
[2] C. K. Ingold, *Structure and Mechanisms in Organic Chemistry*, Cornell University Press, Ithaca, NY **1953**.
[3] D. K. Bohme, L. B. Young, *J. Am. Chem. Soc.* **1970**, *92*, 7354–7358.
[4] H. I. Schiff, D. K. Bohme, *Int. J. Mass Spectrom. Ion Phys.* **1975**, *16*, 167–189.
[5] W. N. Olmstead, J. I. Brauman, *J. Am. Chem. Soc.* **1977**, *99*, 4219–4228.
[6] S. E. Barlow, J. M. V. Doren, V. M. Bierbaum, *J. Am. Chem. Soc.* **1988**, *110*, 7240–7242.
[7] K. Giles, E. P. Grimsrud, *J. Phys. Chem.* **1992**, *96*, 6680–6687.
[8] W. B. Knighton, J. A. Bognar, P. M. Oconnor, E. P. Grimsrud, *J. Am. Chem. Soc.* **1993**, *115*, 12079–12084.
[9] M. N. Glukhovtsev, A. Pross, L. Radom, *J. Am. Chem. Soc.* **1995**, *117*, 2024–2032.
[10] A. A. Viggiano, R. A. Morris, *J. Phys. Chem. A* **1996**, *100*, 19227–19240.
[11] P. Ayotte, J. Kim, J. A. Kelley, S. B. Nielsen, M. A. Johnson, *J. Am. Chem. Soc.* **1999**, *121*, 6950–6951.
[12] L. Sun, K. Song, W. L. Hase, *Science* **2002**, *296*, 875–878.
[13] J. M. Gonzales, C. Pak, R. S. Cox, W. D. Allen, H. F. Schaefer III, A. G. Császár, G. Tarczay, *Chem. Eur. J.* **2003**, *9*, 2173–2192.
[14] J. Mikosch, S. Trippel, C. Eichhorn, R. Otto, U. Lourderaj, J.-X. Zhang, W. L. Hase, M. Weidemüller, R. Wester, *Science* **2008**, *319*, 183–186.
[15] P. Manikandan, J. Zhang, W. L. Hase, *J. Phys. Chem. A* **2012**, *116*, 3061–3080.
[16] C. Hennig, S. Schmatz, *Phys. Chem. Chem. Phys.* **2012**, *14*, 12982–12991.
[17] I. Szabó, A. G. Császár, G. Czakó, *Chem. Sci.* **2013**, *4*, 4362–4370.
[18] J. Xie, R. Otto, J. Mikosch, J. Zhang, R. Wester, W. L. Hase, *Acc. Chem. Res.* **2014**, *47*, 2960–2969.
[19] I. Szabó, G. Czakó, *Nat. Commun.* **2015**, *6*, 5972.
[20] M. Stei, E. Carrascosa, M. A. Kainz, A. H. Kelkar, J. Meyer, I. Szabó, G. Czakó, R. Wester, *Nat. Chem.* **2016**, *8*, 151–156.
[21] J. Xie, W. L. Hase, *Science* **2016**, *352*, 32–33.
[22] Y. Wang, H. Song, I. Szabó, G. Czakó, H. Guo, M. Yang, *J. Phys. Chem. Lett.* **2016**, *7*, 3322–3327.
[23] Y. Li, Y. Wang, D. Y. Wang, *J. Phys. Chem. A* **2017**, *121*, 2773–2779.
[24] I. Szabó, G. Czakó, *J. Phys. Chem. A* **2017**, *121*, 9005–9019.
[25] D. A. Tasi, Z. Fábián, G. Czakó, *Phys. Chem. Chem. Phys.* **2019**, *21*, 7924–7931.
[26] R. Wester, *Mass Spectrom. Rev.* **2022**, *41*, 627–644.
[27] J. Meyer, V. Tajti, E. Carrascosa, T. Győri, M. Stei, T. Michaelsen, B. Bastian, G. Czakó, R. Wester, *Nat. Chem.* **2021**, *13*, 977–981.
[28] D. A. Tasi, G. Czakó, *Chem. Sci.* **2021**, *12*, 14369–14375.
[29] X. Lu, C. Shang, L. Li, R. Chen, B. Fu, X. Xu, D. H. Zhang, *Nat. Commun.* **2022**, *13*, 4427.
[30] X. Lu, L. Li, X. Zhang, B. Fu, X. Xu, D. H. Zhang, *J. Phys. Chem. Lett.* **2022**, *13*, 5253–5259.
[31] S. Zhao, G. Fu, W. Zhen, H. Wang, M. Liu, L. Yang, J. Zhang, *J. Phys. Chem. A* **2023**, *127*, 3381–3389.
[32] A. P. Bento, F. M. Bickelhaupt, *J. Org. Chem.* **2007**, *72*, 2201–2207.
[33] M. A. van Bochove, F. M. Bickelhaupt, *Eur. J. Org. Chem.* **2008**, *2008*, 649–654.
[34] Z.-Z. Yang, Y.-L. Ding, D.-X. Zhao, *J. Phys. Chem. A* **2009**, *113*, 5432–5445.
[35] E. Hupf, M. Olaru, C. I. Rat, M. Fugel, C. B. Hübschle, E. Lork, S. Grabowsky, S. Mebs, J. Beckmann, *Chem. Eur. J.* **2017**, *23*, 10568–10579.
[36] T. A. Hamlin, M. Swart, F. M. Bickelhaupt, *ChemPhysChem* **2018**, *19*, 1315–1330.

[37] M. Fugel, A. Dittmer, F. Kleemiss, S. Grabowsky, *J. Phys. Chem. A* **2021**, *125*, 4070–4078.
[38] A. Á. Dékány, G. Z. Kovács, G. Czakó, *J. Phys. Chem. A* **2021**, *125*, 9645–9657.
[39] A. Á. Dékány, G. Czakó, *J. Chem. Phys.* **2023**, *158*, 224303.
[40] M. Bühl, H. F. Schaefer III, *J. Am. Chem. Soc.* **1993**, *115*, 9143–9147.
[41] R. Gareyev, S. Kato, V. M. Bierbaum, *J. Am. Soc. Mass Spectrom.* **2001**, *12*, 139–143.
[42] J. Lv, J. Zhang, D. A. Wang, *Phys. Chem. Chem. Phys.* **2016**, *18*, 6146–6152.
[43] X. Liu, C. Zhao, L. Yang, J. Zhang, R. Sun, *Phys. Chem. Chem. Phys.* **2017**, *19*, 22691–22699.
[44] J. Kubelka, F. M. Bickelhaupt, *J. Phys. Chem. A* **2017**, *121*, 885–891.
[45] B. Hajdu, G. Czakó, *J. Phys. Chem. A* **2018**, *122*, 1886–1895.
[46] D. Papp, G. Czakó, *Chem. Sci.* **2021**, *12*, 5410–5418.
[47] M. A. van Bochove, M. Swart, F. M. Bickelhaupt, *J. Am. Chem. Soc.* **2006**, *128*, 10738–10744.
[48] M. A. van Bochove, M. Swart, F. M. Bickelhaupt, *ChemPhysChem* **2007**, *8*, 2452–2463.
[49] O. I. Kolodiazhnyi, A. Kolodiazhna, *Tetrahedron: Asymmetry* **2017**, *28*, 1651–1674.
[50] B. J. Braams, J. M. Bowman, *Int. Rev. Phys. Chem.* **2009**, *28*, 577–606.
[51] K. Raghavachari, G. W. Trucks, J. A. Pople, M. Head-Gordon, *Chem. Phys. Lett.* **1989**, *157*, 479–483.
[52] T. H. Dunning Jr., *J. Chem. Phys.* **1989**, *90*, 1007–1023.
[53] R. Welsch, U. Manthe, *J. Chem. Phys.* **2013**, *138*, 164118.
[54] T. Győri, G. Czakó, *J. Chem. Theory Comput.* **2020**, *16*, 51–66.
[55] G. Czakó, T. Győri, D. Papp, V. Tajti, D. A. Tasi, *J. Phys. Chem. A* **2021**, *125*, 2385–2393.
[56] S. Yabushita, M. S. Gordon, *Chem. Phys. Lett.* **1985**, *117*, 321–325.
[57] J. M. Denu, D. L. Lohse, J. Vijayalakshmi, M. A. Saper, J. E. Dixon, *Proc. Natl. Acad. Sci. USA* **1996**, *93*, 2493–2498.
[58] M. Oivanen, S. Kuusela, H. Lönnberg, *Chem. Rev.* **1998**, *98*, 961–990.
[59] S. D. Lahiri, G. Zhang, D. Dunaway-Mariano, K. N. Allen, *Science* **2003**, *299*, 2067–2071.
[60] D. A. Tasi, T. Győri, G. Czakó, *Phys. Chem. Chem. Phys.* **2020**, *22*, 3775–3778.
[61] T. B. Adler, G. Knizia, H.-J. Werner, *J. Chem. Phys.* **2007**, *127*, 221106.
[62] K. A. Peterson, T. H. Dunning Jr., *J. Chem. Phys.* **2002**, *117*, 10548–10560.
[63] MOLPRO, version 2015.1, a package of ab initio programs, H.-J. Werner, P. J. Knowles, G. Knizia, F. R. Manby, M. Schütz, P. Celani, W. Györffy, D. Kats, T. Korona, R. Lindh *et al.*, see http://www.molpro.net.
[64] K. A. Brueckner, *Phys. Rev.* **1954**, *96*, 508–516.
[65] W. L. Hase, *Encyclopedia of Computational Chemistry*, Wiley, New York **1998**, pp. 399–407.
[66] G. Czakó, B. C. Shepler, B. J. Braams, J. M. Bowman, *J. Chem. Phys.* **2009**, *130*, 084301.

Manuscript received: July 3, 2023
Version of record online: September 12, 2023